Iryna Didych, Oleh Yasniy, Dmytro Tymoshchuk, Oleksandr Holotenko, Viktor Boichun*

COMPARATIVE ANALYSIS OF THE ACCURACY OF NEURAL NETWORK AND ANALYTICAL METHODS IN MODELLING FATIGUE FRACTURE OF TITANIUM ALLOY

UPOREDNA ANALIZA TAČNOSTI NEURONSKE MREŽE I ANALITIČKIH METODA U MODELIRANJU ZAMORNOG LOMA TITANIJUMSKE LEGURE

Originalni naučni rad / Original scientific paper
Rad primljen / Paper received:
https://doi.org/10.69644/ivk-2026-siA-0015
Adresa autora / Author's address:
Department of Computer-Integrated Technologies, Ternopil Ivan Puluj National Technical University, Ternopil, Ukraine

*email: iryna.didych1101@gmail.com
I. Didych https://orcid.org/0000-0003-2846-6040 ;
O. Yasniy https://orcid.org/0000-0002-9820-9093 ;
D. Tymoshchuk https://orcid.org/0000-0003-0246-2236 ;
O. Holotenko https://orcid.org/0000-0001-9251-8760 ;
V. Boichun https://orcid.org/0009-0008-5540-5431

Keywords
- fatigue crack growth rate
- artificial intelligence
- machine learning
- boosted trees

Abstract

Fatigue crack growth rate is modelled by neural network and compared with analytical models, namely, the Paris' law and polynomial log regressions of the second to fifth degree. To assess the accuracy of the modelling, the determination coefficient R^2, mean absolute error (MAE) and mean absolute percentage error (MAPE) are used to assess the accuracy of the modelling. Results show that both approaches, in particular, the classical analytical models and the neural network, provide the high accuracy of approximation of the experimental data. At the same time, the neural network demonstrates an advantage in the region of high values of ΔK, where a nonlinear acceleration of crack growth is observed, reaching a coefficient of determination R^2 equal to 0.9994. The presented approach confirms the effectiveness of applying machine learning methods, in particular neural networks, in the problems of fracture mechanics and fatigue analysis.

Ključne reči
- brzina rasta zamorne prsline
- veštačka inteligencija
- mašinsko učenje
- potpomognuta stabla odlučivanja

Izvod

U ovom radu izvodi se modeliranje brzina rasta zamorne prsline pomoću neuronske mreže i upoređuje sa analitičkim modelima, odnosno Parisovim zakonom i polinomijalnim log-regresijama drugog do petog stepena. Za procenu tačnosti modeliranja korišćeni su koeficijent determinacije R^2, srednja apsolutna greška (MAE) i srednja apsolutna procentualna greška (MAPE). Rezultati pokazuju da oba pristupa, posebno klasični analitički modeli i neuronska mreža, obezbeđuju veliku tačnost aproksimacije eksperimentalnih podataka. Istovremeno, neuronska mreža je pokazala prednost u oblasti visokih vrednosti ΔK, gde se uočava nelinearno ubrzanje rasta prsline, dostižući koeficijent determinacije R^2 u iznosu 0,9994. Predstavljeni pristup potvrđuje efikasnost primene metoda mašinskog učenja, posebno neuronskih mreža, u problemima mehanike loma i analize zamora.

INTRODUCTION

The problem of material fatigue and fatigue crack growth prediction is relevant for ensuring the reliability of engineering structures. Fatigue failure occurs gradually: a crack formed under cyclic loads increases with each cycle until the structure loses its integrity. To evaluate the service life of parts, fracture mechanics approaches are traditionally used /1/, in particular, the dependence of the fatigue crack growth (FCG) rate da/dN on the stress intensity factor (SIF) range $\Delta K = K_{max} - K_{min}$, where K_{max}, K_{min} are the maximum and minimum stress intensity factors of the loading cycle, respectively. At the same time, the stress ratio $R = K_{min}/K_{max}$ significantly affects the FCG (Fig. 1). The Paris law is a classical one /2/. However, it describes the second area of the FCG diagram and does not account for the influence of several factors, such as the stress ratio R, /3/.

There are numerous modifications of Paris's law that extend its applicability to other regions and loading conditions /4-5/. However, even improved analytical models may not fully account for the complex nonlinearity of crack growth under variable conditions.

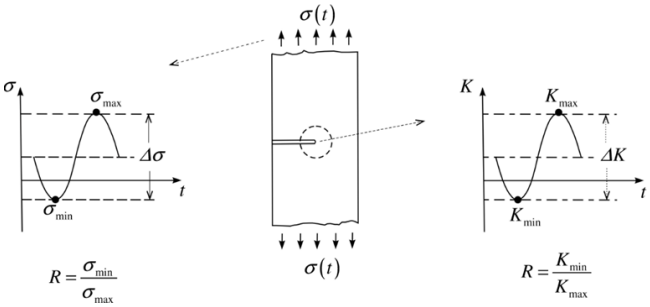

Figure 1. Loading and cyclic stress intensity factor relation, /3/.

In this regard, approaches based on machine learning, in particular artificial neural networks, are gaining increasing attention. Neural networks can approximate complex nonlinear dependencies and account for multiple factors simultaneously, making them promising for predicting crack growth. In particular, the authors of article /6/ propose using artificial neural networks to predict FCG under variable loads in aircraft structures, demonstrating their ability to reproduce complex load spectra with high accuracy. The authors

in /7/ investigate the effectiveness of new parameters of the fatigue crack growth driving force, namely, K_{max} and ΔK^{+}, to describe the influence of the stress ratio R on the crack growth rate, showing that these parameters are not inferior to or superior to the traditional approach based on ΔK. The authors in /8/ investigate the use of an artificial neural network to predict FCG in aluminium alloys, demonstrating a high correlation between the model results and experimental data. Meanwhile, the authors of article /9/ use optimised neural networks (based on a genetic algorithm, hill climbing, and simulated annealing) to predict the growth rate of fatigue cracks in aviation aluminium alloys, achieving high modelling accuracy and consistency with experimental data. The authors in /10/ use machine learning methods to model the fatigue life of automotive steel, demonstrating the effectiveness in the approach of predicting the material's durability under cyclic loading. The authors of article /11/ build a neural network model to predict FCG rate in titanium alloys as a function of the number of load cycles and the asymmetry coefficient, achieving high accuracy (error up to 0.4 %) and adaptability across different load modes. In article /12/ the authors propose an incremental learning scheme based on a fully connected neural network for predicting fatigue crack growth in aluminium and titanium alloy specimens, demonstrating the superiority of the proposed approach over traditional approximation methods and popular neural network architectures, RNNs and LSTMs in particular. The authors in /13/ propose a method for predicting fatigue crack growth by correcting a machine learning model with actual data, thereby increasing model accuracy and adaptability in changing load conditions, including multistage and mixed loads. The authors of article /14/ develop neural network models for real-time prediction of the residual life of structures under uncertainty, comparing five NN architectures and showing that the 'H1-L1' model achieves the best accuracy with the least training data, making it promising for technical condition monitoring. The authors in /15/ propose a new approach to predicting fatigue crack growth in aluminium alloys based on a spatio-temporal neural network (SimVP STNN) that processes images from digital image correlation (DIC) and provides high accuracy in predicting cracks without the need for traditional modelling or computational mechanics. Authors in /16/ apply a machine learning algorithm based on backpropagation of error to predict the growth rate of fatigue cracks in nickel superalloys GTM 720 and GTM 718, focusing on the Paris region and demonstrating good agreement between the predictions and experimental data at different stress ratios. The authors of article /17/ compare three machine learning algorithms, that is, extreme learning machine (ELM), radial basis function network (RBFN), and optimised backpropagation network with genetic algorithm (GABP) in the task of predicting fatigue crack growth, showing that ML approaches outperform classical models, and ELM provides the best accuracy and extrapolation ability. The authors of article /18/ propose an approach to predicting the fatigue failure lifetime of three-dimensional specimens with cracks using a backpropagated neural network that reproduces the relationship between the crack growth rate and the effective SIF range with high accuracy. The authors in /19/ develop a method for detecting FGC in real time based on a combination of computer vision and machine learning, with the decision-making model achieving the highest classification accuracy and a crack length measurement accuracy of 0.6 mm.

The application of machine learning methods extends far beyond fracture mechanics and crack growth prediction. Thus, the authors in /20/ consider the application of ML algorithms for the classification of composite materials, and in /21/, artificial intelligence is successfully applied to the identification of epoxy composites for aviation. Meanwhile, in /22/ the authors investigate the effect of a metal filler on the mechanical properties of epoxy resin and based on the analysis of experimental results, they find that its addition can increase the strength and stiffness of the composite. In addition, machine learning is widely used in materials science. Article /23/ provides an overview of the use of boosting algorithms for analysing, predicting properties, and optimising the composition of polymers, demonstrating the high effectiveness of such approaches in solving complex problems in materials science. Additionally, in some studies /24-25/, machine learning is used to model the hysteretic behaviour of shape memory alloys, accounting for the frequency of load cycles. In the field of intelligent material modelling, machine learning is also actively used to describe the dynamic behaviour of smart materials. For example, the authors in /26/ demonstrate the use of an ML approach to model the dynamic response of superelastic shape memory alloys, enabling effective reproduction of complex nonlinearities in the behaviour of SMA wires under cyclic loading. In the field of environmental monitoring, the authors of /27-28/ demonstrate the effectiveness of ML algorithms for predicting atmospheric pollutant concentrations, such as CO, based on related parameters. All these examples confirm the versatility of artificial intelligence methods and their ability to successfully solve complex problems in a wide variety of application areas.

The paper presents a comparative analysis of analytical models (Paris' empirical law and polynomial approximations of various degrees) and an artificial neural network model for modelling the FCG rate in a titanium alloy. The aim of the study is to evaluate the accuracy of the neural network and traditional approaches. To quantitatively assess the models' accuracy, the metrics mean absolute error (MAE), mean square error (MSE), mean absolute relative error (MAPE), and coefficient of determination (R^2) are used.

MATERIAL AND METHODS

Analytical models of crack growth

The Paris-Erdoğan law /2/ is traditionally used to model the mid section of the FCG diagram. This law postulates a power relationship between the FCG rate *da/dN* and the SIF range ΔK:

$$\frac{da}{dN} = C(\Delta K)^m , \tag{1}$$

where: *da/dN* is FCG rate; *a* is crack length; *N* is number of loading cycles; ΔK is SIF range; *C* and *m* are empirically determined material constants.

Paris' law effectively describes the stable part (region II) of the FCG diagram but shows limitations at the boundaries of the ΔK range, particularly near the growth threshold and in the accelerated growth region. In this study, the values of parameters C and m are selected for a specific material and a set of experimental conditions, enabling the derivation of a basic two-parameter description of the FCG process.

In addition to the power model, the approximation of the dependence of da/dN on ΔK using polynomials in logarithmic coordinates /29/ is considered. In other words, the curve $\log_{10}(da/dN)$ is approximated as a polynomial of $\log_{10}(\Delta K)$. Polynomials of various degrees are used in the study: quadratic (degree 2, denoted Quad), cubic (degree 3, denoted Cubic), fourth degree (Deg4), and fifth degree (Deg5). The general form of such a polynomial model is as follows:

$$\log_{10}\left(\frac{da}{dN}\right)=a_0+a_1\log_{10}(\Delta K)+a_2(\log_{10}(\Delta K))^2+ \\ +\ldots+a_n(\log_{10}(\Delta K))^n, \quad (2)$$

where: a_0, a_1, …, a_n are polynomial coefficients; n is the degree of the polynomial approximation.

Polynomial models allow for flexible approximation of experimental dependence, especially outside the scope of strict compliance with Paris' law. Increasing the degree of the polynomial theoretically improves the fit to the available data, though at excessively high degrees, overfitting may occur, i.e., the model begins to describe noise in the data rather than the underlying pattern.

Neural networks (MLP)

Artificial neural networks (ANNs) are powerful machine learning tools that mimic the architecture and functional principles of biological neural systems /30-31/. They consist of layers of interconnected neurons that transform input signals into output values by learning weight coefficients based on data. Due to their ability to model complex nonlinear functions, NNs effectively reveal hidden patterns even in large and heterogeneous datasets without requiring *a priori* determination of the analytical form of the dependence. This property is especially valuable when working with experimental fatigue data, which is often noisy or incomplete. In addition, neural networks offer strong generalisation and can accommodate additional parameters, thereby expanding their use in predicting fatigue life and residual strength of structures. These advantages drive the growing popularity of neural networks in fracture mechanics, materials science, and related engineering disciplines. The general architecture of a multilayer perceptron (MLP) for such tasks is shown in Fig. 2.

The network includes input neurons corresponding to the main features of the experimental data, hidden layers of neurons with the nonlinear ReLU activation function, and an output neuron with a linear activation function to produce a continuous prediction value. Signals are transmitted between layers through a system of weight coefficients, which are optimised during network training to minimise the loss function. This architecture provides an effective approximation of complex nonlinear dependencies between input parameters and the target variable, which is characteristic of experimental data analysis tasks in materials mechanics and FCG parameter prediction.

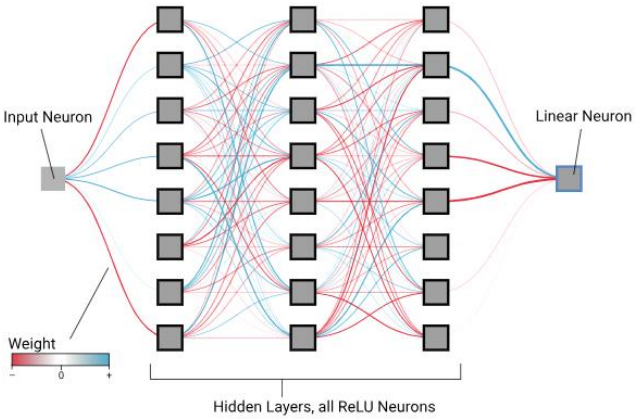

Figure 2. Architecture of a multilayer artificial neural network of the multilayer perceptron (MLP) type with hidden layers, /32/.

This study uses an MLP neural network implemented based on the TensorFlow/Keras library. The model architecture is dynamically constructed using an automated hyperparameter selection procedure. The network's input layer accepts a feature vector corresponding to the number of input parameters in the experimental data. The first hidden layer contains 32-256 neurons, determined during the optimisation process. L2 regularization is applied to the weight coefficients to prevent overfitting. The ReLU activation function is used in each hidden layer, which ensures stable training of deep neural networks and reduces the problem of gradient decay. After each dense layer, Batch Normalisation and Dropout are applied to stabilise the learning process and improve the model's generalisation. The probability of neuron dropout in the Dropout layer ranged from 0.1 to 0.2.

The number of additional hidden layers is treated as a hyperparameter and could range from 1 to 2. For each layer, the number of neurons is optimised over 32-256.

Network parameter optimisation is performed using the Adam algorithm which provides adaptive learning rate adjustment. The learning rate value is considered a hyperparameter. The loss function is the mean squared error (MSE). The Keras Tuner RandomSearch tool is used for automatic hyperparameter selection, which performs a random search in each parameter space. During the optimisation process, 500 independent trials are conducted, each corresponding to a different model architecture configuration. During each trial, the model is trained for up to 300 epochs, with 10 % of the training sample used for validation.

To prevent overfitting, the Early Stopping mechanism is used, which stops training when validation error does not improve for 150 epochs. After completing the optimisation procedure, the model with the lowest validation loss function value is selected.

The best model configuration is additionally trained on the training data for up to 1300 epochs using Early Stopping (patience = 150) and Model Checkpoint mechanisms, which store the model weights with the best validation error. This approach enabled us to obtain a final model with optimal parameters and strong generalisation.

Model evaluation metrics

Several standard regression error metrics are used to quantitatively assess the accuracy and quality of the models: mean

absolute error (MAE), mean squared error (MSE), mean absolute percentage error (MAPE), and coefficient of determination (R^2) allowed us to obtain a more complete and objective characterisation of the model's performance. Each of these metrics reflects different aspects of forecast quality, namely accuracy in physical units, stability, relative deviations, and the model's ability to explain variation in the data. This comprehensive approach increases the reliability of conclusions about each method's effectiveness.

Mean absolute error (MAE): the average value of the difference between the predicted and actual values:

$$\mathrm{MAE} = \frac{1}{n}\sum_{i=1}^{n}\left|y_{true}^{test}(i) - y_{pred.}^{test}(i)\right|, \quad (3)$$

where: $y_{true}^{test}(i)$ is experimental value of the sample element in the test data set; $y_{pred.}^{test}(i)$ is predicted sample element in the test data set; n is test data set size.

Mean squared error (MSE): the average value of the square of the difference between the forecast and the actual value:

$$\mathrm{MSE} = \frac{1}{n}\sum_{i=1}^{n}\left(y_{true}^{test}(i) - y_{pred.}^{test}(i)\right)^2. \quad (4)$$

Mean absolute percentage error (MAPE): average percentage deviation of the forecast from the actual value (in absolute values):

$$\mathrm{MAPE} = \frac{1}{n}\sum_{i=1}^{n}\frac{\left|y_{true}^{test}(i) - y_{pred.}^{test}(i)\right|}{\left|y_{true}^{test}(i)\right|}\cdot 100\%. \quad (5)$$

Coefficient of determination R_2: an indicator that reflects the proportion of variance in the dependent variable explained by the model. It is calculated as:

$$R^2 = 1 - \frac{\sum_{i=1}^{n}\left(y_{true}^{test}(i) - y_{pred.}^{test}(i)\right)^2}{\sum_{i=1}^{n}\left(y_{true}^{test}(i) - \bar{y}_{pred.}^{test}\right)^2}, \quad (6)$$

where: $\bar{y}_{pred.}^{test}$ is the mean value of experimental data.

RESULTS AND DISCUSSION

In this paper, the FCG rate is modelled by a neural network at stress ratio $R = 0.03$. The sample contained 154 elements /33/, of which 70 % are randomly selected for the training set, and 30 % are left to evaluate the quality of the prediction. Figure 3 shows the change in loss function values as a function of the number of epochs during neural network training to predict the FCG rate at a stress ratio of $R = 0.03$. The purple curve shows loss function values on the training sample, while the red curve shows the values on the validation sample. During the training process, both curves show stable changes with minor fluctuations, reflecting the stochastic nature of network parameter optimisation. At the same time, the loss values on the validation sample remain lower than those on the training sample, indicating the model good generalisation ability. Despite the fluctuation characteristic of the neural network training process, the overall stability of the curves confirms the effectiveness of the chosen architecture and training parameters. By the end of the training process, approximately 800-900 epochs, the loss function values stabilise, indicating that the model has converged.

Figure 4 shows the relationship between experimental FCG rate and corresponding neural network predictions for the test sample at stress ratio $R = 0.03$. Black marks (asterisks) illustrate 'fact-prediction' pairs, and the orange line reflects the ideal match. Importantly, the proximity of the points along this diagonal indicates the model's high predictive accuracy. Deviations from the straight line are minimal across the entire range of values, confirming the absence of systematic errors and the model's ability to generalise beyond the training data.

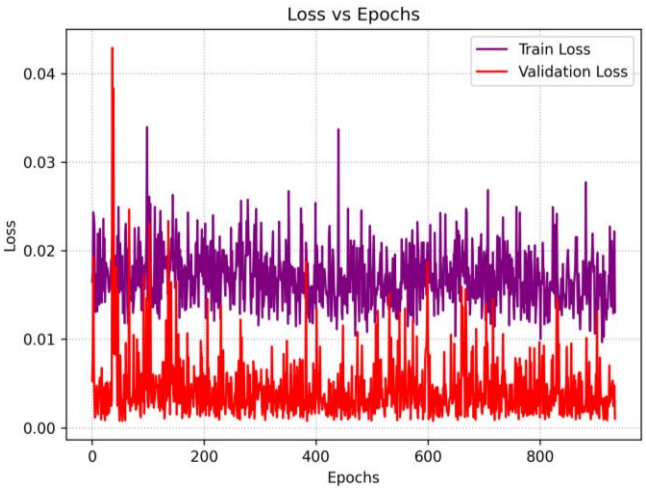

Figure 3. Dynamics of the loss function during neural network training at $R = 0.03$.

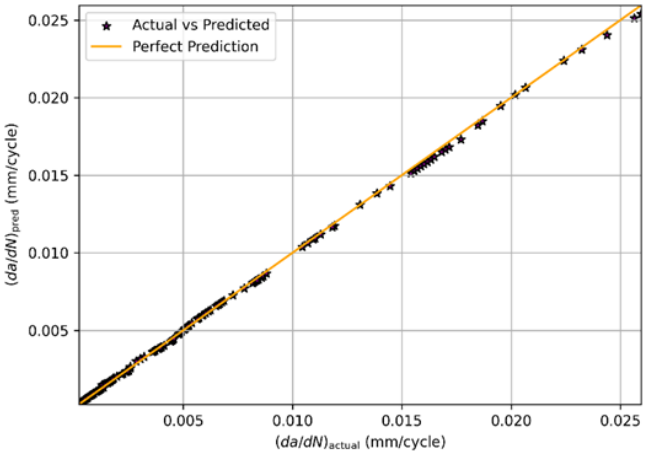

Figure 4. Predicted and experimental values of FCG rate, obtained by method of neural networks.

Figure 5 shows dependence of fatigue crack growth rate da/dN on stress intensity factor range ΔK in normal coordinates. Figure 5a shows an exact match between experimental values and those obtained using a neural network. The prediction curve closely reproduces the shape of the experimental dependence over the entire ΔK interval studied. Figure 5b compares analytical approximations of different orders (Paris' law, quadratic, cubic, and 4th and 5th degree polynomials). All models agree well with the experiment in the middle range of ΔK, but the highest accuracy across the entire curve is achieved with higher-degree polynomials (Deg4, Deg5), as confirmed by the high R^2 values.

For a more detailed analysis of the nature of the dependence and assessment of the conformity of results with classical fracture mechanics models, this dependence is also presented in double logarithmic coordinates (Fig. 6). In this

representation, the nature of the change in crack growth rate and the linearity of the dependence in the Paris range are more clearly traced, which allows a visual comparison of experimental results with model predictions and analytical approximations.

Table 1 presents analytical expressions for polynomial models constructed on a logarithmic scale to approximate the dependence of fatigue crack growth rate on the stress intensity factor range ΔK. The dependence is presented as second- to fifth-degree polynomials of $\log_{10}(\Delta K)$, which gradually increase the function's flexibility and improve its ability to reproduce characteristic sections of the crack growth curve.

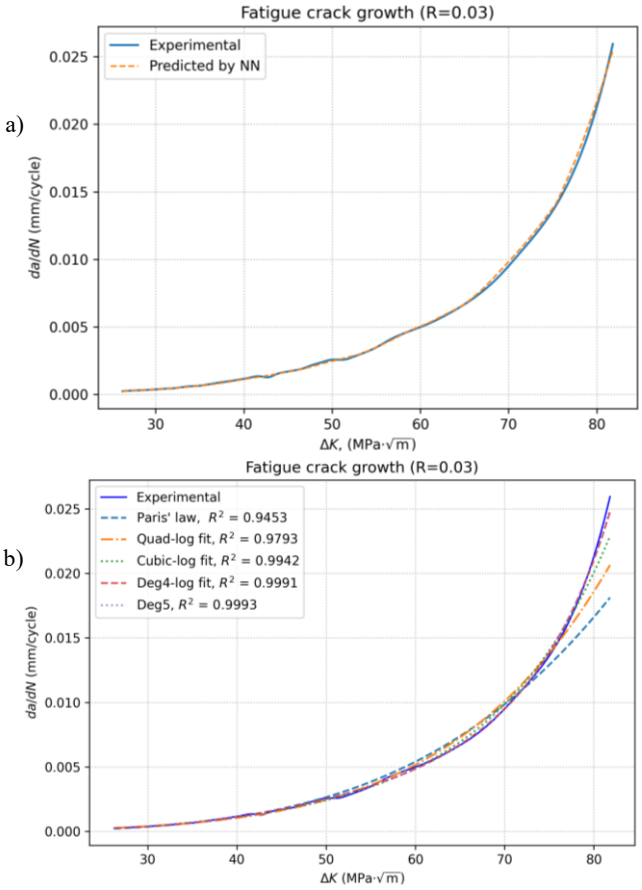

Figure 5. Predicted and experimental dependences of FCG rate on the ΔK for $R = 0.03$ in linear coordinates: a) by method of neural networks; and b) analytical methods.

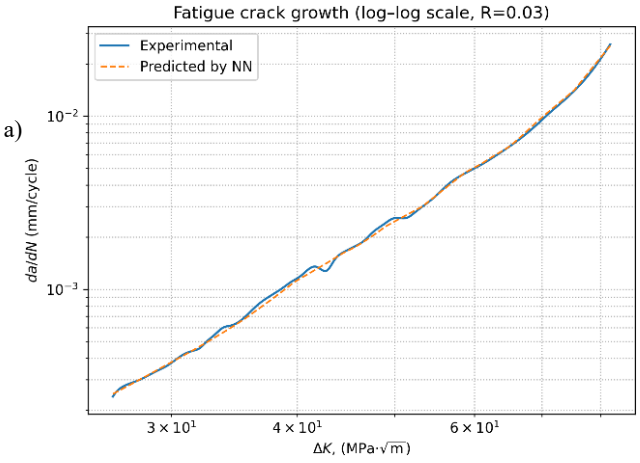

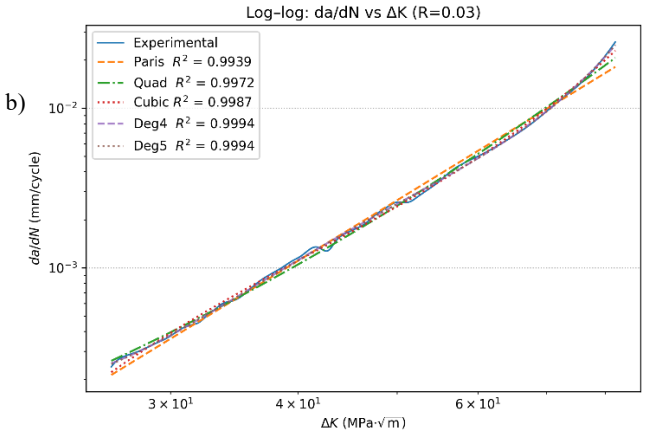

Figure 6. Predicted and experimental dependences of FCG rate on ΔK for $R = 0.03$ in log-log coordinates by: a) neural networks; and b) analytical methods.

Table 1. Polynomial models for logarithmic dependence $\log_{10}(da/dN)$ on $\log_{10}(\Delta K)$.

Models	Equations
Paris' law	$\frac{da}{dN} = 6.094\times10^{-10}(\Delta K)^{3.907}$
Quad	$\log_{10}\left(\frac{da}{dN}\right) = -4.2674 - 2.0087\log_{10}(\Delta K) + +1.7599(\log_{10}(\Delta K))^2$
Cubic	$\log_{10}\left(\frac{da}{dN}\right) = -48.528 + 77.831\log_{10}(\Delta K) - -46.038(\log_{10}(\Delta K))^2 + 9.4955(\log_{10}(\Delta K))^3$
Deg4	$\log_{10}\left(\frac{da}{dN}\right) = 356.93 - 899.871\log_{10}(\Delta K) + 835.22\times \times(\log_{10}(\Delta K))^2 - 342.43(\log_{10}(\Delta K))^3 + 52.538(\log_{10}(\Delta K))^4$
Deg5	$\log_{10}\left(\frac{da}{dN}\right) = -43.845 + 309.89\log_{10}(\Delta K) - -621.86(\log_{10}(\Delta K))^2 + 532.88(\log_{10}(\Delta K))^3 - -209.73(\log_{10}(\Delta K))^4 + 31.357(\log_{10}(\Delta K))^5$

As shown in Table 1, each subsequent increase in the degree of the polynomial allows the model to describe the experimental data more accurately, especially in nonlinear regions, particularly in the threshold growth region and the accelerated failure zone. This approach provides a more accurate representation of complex dependence than the classical power model and can serve as an effective tool for interpolation and limited extrapolation.

These polynomial models allow for flexible approximation of experimental dependence, especially outside the region of strict compliance with Paris' law. Increasing the degree of the polynomial theoretically improves the fit to the available data, though at excessively high degrees, overfitting may occur, and the model begins to describe noise in the data rather than the underlying pattern.

Table 2 presents a quantitative assessment of the models' accuracy. Paris's law provides a coefficient of determination of 0.945, i.e., it explains 94.5 % of the variance in the experimental data. Improving this indicator to 0.979 gives a quadratic polynomial model, and a cubic model gives 0.994, which is close to 100 %. Polynomials of 4th and 5th degrees further increase R^2 to 0.9991-0.9993 and reduce the average MAPE error by 2.3 %. In fact, Deg5 minimises the RMSE, corresponding to an average deviation of only 0.000095

mm/cycle. In terms of these metrics, the 5th degree polynomial is the best of analytical models. However, one should be aware of its shortcomings, in particular, overfitting. Importantly, the neural network demonstrates the ability to generalise, i.e., its errors on delayed data remaining low, whereas the 5th-degree polynomial could potentially yield significantly larger deviations when encountering new data outside the training range. In other words, the neural network is less prone to overfitting due to regularisation (Dropout), and its model smoothly interpolates a physically meaningful curve.

Table 2. Comparison of the accuracy of crack growth rate prediction models.

Models/prediction errors	MSE	MAE	R^2	MAPE (%)
Paris' law	1.996e-06	0.00062	0.9453	7.43
Quad	7.537e-07	0.00039	0.9793	5.40
Cubic	2.111e-07	0.00022	0.9942	3.78
Deg4	3.145e-08	0.00010	0.9991	2.29
Deg5	2.504e-08	0.00009	0.9993	2.28
Neural network MLP	0.01515	0.07894	0.99931	5.32

As shown in Table 2, the neural network achieved an R^2 of 0.9993 and an average relative error of 5.3 %. Network accuracy is slightly inferior to the Deg5 polynomial on the training data, as expected, due to the targeted regularisation that helps avoid overfitting; the model did not attempt to pass through all points perfectly. As a result, the network has a smoother forecast. It should be noted that the difference in MAPE between NN and Deg5 is small, so in the context of engineering calculations, both approaches can be considered sufficiently accurate for practical use. However, the neural network model should be preferred due to its stability at the edges of the ΔK range and flexibility.

Polynomial models have demonstrated that increasing the degree of the polynomial achieves the accuracy of a neural network. Polynomials of the 4th and 5th degrees are not inferior to neural networks on the training sample. This indicates that, for interpolation within the studied range, high-degree polynomials can serve as an alternative to neural networks, as they can also adapt to complex curve shapes. At the same time, it is important to consider the risks of modelling too high an order. A 5th-degree polynomial provides an excellent fit to the available data, but such models can be overtrained: the slightest extrapolation outside the data range or the influence of random noise can lead to significant errors. Thanks to regularisation methods (dropout, batch normalisation), neural networks are less prone to overfitting, although this also depends on the amount of data and training settings. In addition, neural networks are more versatile: they can be retrained or further trained to account for additional influencing factors, such as stress ratios and material properties, whereas a polynomial model would require a fundamentally different form of dependence to accommodate new variables.

CONCLUSIONS

The paper compares the effectiveness of classical analytical approaches and the neural network method in modelling the fatigue crack growth (FCG) rate of titanium alloys. Paris' law, being the simplest model, shows high accuracy on experimental data, while providing a basic approximation and physically interpretable parameters. Polynomial models significantly improve the fit, especially the 4th- and 5th-order models, which achieve the same level of accuracy as the neural network. The artificial neural network achieves the highest prediction accuracy, with a coefficient of determination $R^2 > 0.999$, thanks to its ability to capture nonlinear dependencies without specifying their explicit form. It demonstrates an advantage in the high ΔK regime, where nonlinear crack growth acceleration is observed, a region traditionally difficult to approximate with classical models. Thus, the application of machine learning methods has proven as effective for FCG prediction and fatigue analysis in general.

Thus, neural networks are a promising tool for predicting FCG, especially when high accuracy and consideration of complex factors are required. High-degree polynomial approximations can achieve similar accuracy on available data, but risk losing it when extrapolating or in the presence of noise. In practical applications, it is advisable to combine these approaches: use physically based models for initial estimates and process understanding; and use flexible machine learning models for accurate predictions and sensitivity analysis. This will ensure both reliability and comprehensibility of the model, as well as high accuracy in predicting the residual life of materials.

REFERENCES

1. Varfolomeev, I.V., Yasnii, O.P. (2008), *Modeling of fracture of cracked structural elements with the use of probabilistic methods*, Mater. Sci. 44(1): 87-96. doi: 10.1007/s11003-008-9047-5
2. Paris, P.C., Erdogan, F.A. (1963), *Critical analysis of crack propagation laws*, J Basic Eng. 85(4): 528-534. doi: 10.1115/1.3656900
3. Kuna, M., Finite Elements in Fracture Mechanics: Theory - Numerics - Applications, Springer Dordrecht, 2013. doi: 10.1007/978-94-007-6680-8
4. Forman, R.G., Kearney, V.E., Engle, R.M. (1967), *Numerical analysis of crack propagation in cyclic-loaded structures*, J Basic Eng. 89(3): 459-463. doi: 10.1115/1.3609637
5. Elber, W. (1970), *Fatigue crack closure under cyclic tension*, Eng. Fract. Mech. 2(1): 37-45. doi: 10.1016/0013-7944(70)90028-7
6. Pidaparti, R.M.V., Palakal, M.J. (1995), *Neural network approach to fatigue-crack-growth predictions under aircraft spectrum loadings*, J Aircraft, 32(4): 825-831. doi: 10.2514/3.46797
7. Dinda, S., Kujawski, D. (2004), *Correlation and prediction of fatigue crack growth for different R-ratios using K_{max} and ΔK^+ parameters*, Eng. Fract. Mech. 71(12): 1779-1790. doi: 10.1016/j.engfracmech.2003.06.001
8. Mohanty, J.R., Verma, B.B., Parhi, D.R.K., Ray, P.K. (2009), *Application of artificial neural network for predicting fatigue crack propagation life of aluminum alloys*, Arch. Comput. Mater. Sci. Surf. Eng. 1(3): 133-138.
9. Younis, H.B., Kamal, K., Sheikh, M.F., Hamza, A. (2022), *Prediction of fatigue crack growth rate in aircraft aluminum alloys using optimized neural networks*, Theor. Appl. Fract. Mech. 117: 103196. doi: 10.1016/j.tafmec.2021.103196
10. Yasniy, O., Tymoshchuk, D., Didych, I., et al. (2024), *Modelling of automotive steel fatigue lifetime by machine learning method*, ITTAP'2024: 4th Int. Workshop on Information Technologies: Theoretical and Applied Problems, 2024, Ternopil, Ukraine, Opole, Poland, CEUR Workshop Proc., 3896: 165-172.

11. Yasniy, O., Didych, I., Tymoshchuk, D., et al. (2025), *Prediction of structural elements lifetime of titanium alloy using neural network*, Procedia Struct. Integr. 72: 181-187. doi: 10.1016/j.prostr.2025.08.090
12. Ma, X., He, X., Tu, Z.C. (2021), *Prediction of fatigue-crack growth with neural network-based increment learning scheme*, Eng. Fract. Mech., 241: 107402. doi: 10.1016/j.engfracmech.2020.107402
13. Fang, X., Liu, G., Wang, H., et al. (2022), *Fatigue crack growth prediction method based on machine learning model correction*, Ocean Eng. 266(Part 4): 112996. doi: 10.1016/j.oceaneng.2022.112996
14. Giannella, V., Bardozzo, F., Postiglione, A., et al. (2023), *Neural networks for fatigue crack propagation predictions in real-time under uncertainty*, Comput. Struct. 288: 107157. doi: 10.1016/j.compstruc.2023.107157
15. Liang, J.M., Yu, Y., Hu, Y.L., et al. (2024), *Image-driven prediction of fatigue crack growth in metal materials via spatio-temporal neural network*, Eng. Fract. Mech. 310: 110442. doi: 10.1016/j.engfracmech.2024.110442
16. Mahesh, S., Anil Chandra, A.R., Kumar, L.R., Manjunatha, C.M. (2024), *Fatigue crack growth rate prediction in nickel-based super-alloys using machine learning algorithm*, Procedia Struct. Integr. 60: 382-389. doi: 10.1016/j.prostr.2024.05.059
17. Wang, H., Zhang, W., Sun, F., Zhang, W. (2017), *A comparison study of machine learning based algorithms for fatigue crack growth calculation*, Materials, 10(5): 543. doi: 10.3390/ma10050543
18. Zhang, J., Zhu, J., Guo, W., Guo, W. (2022), *A machine learning-based approach to predict the fatigue life of three-dimensional cracked specimens*, Int. J Fatigue, 159: 106808. doi: 10.1016/j.ijfatigue.2022.106808
19. Zhang, L., Wang, Z., Wang, L., et al. (2021), *Machine learning based real-time visible fatigue crack growth detection*, Digit. Comm. Netw. 7(4): 551-558. doi: 10.1016/j.dcan.2021.03.003
20. Tymoshchuk, D., Didych, I., Maruschak, P., et al. (2025), *Machine learning approaches for classification of composite materials*, Modelling, 6(4): 118. doi: 10.3390/modelling6040118
21. Yasniy, O., Maruschak, P., Mykytyshyn, A., et al. (2025), *Artificial intelligence as applied to classifying epoxy composites for aircraft*, Aviation, 29(1): 22-29. doi: 10.3846/aviation.2025.23149
22. Bhavith, K., Prashanth, P.M., Sudheer, M., et al. (2023), *The effect of metal filler on the mechanical performance of epoxy resin composites*, Eng. Proc. 59(1): 200. doi: 10.3390/engproc2023059200
23. Malashin, I., Tynchenko, V., Gantimurov, A., et al. (2025), *Boosting-based machine learning applications in polymer science: A review*, Polymers, 17(4): 499. doi: 10.3390/polym17040499
24. Yasniy, O., Tymoshchuk, D., Didych, I., et al. (2025), *Modeling of shape memory alloys hysteresis behavior considering the loading cycle frequency*, Procedia Struct. Integr. 72: 188-194. doi: 10.1016/j.prostr.2025.08.091
25. Tymoshchuk, D., Yasniy, O., Maruschak, P., et al. (2024), *Loading frequency classification in shape memory alloys: A machine learning approach*, Computers, 13(12): 339. doi: 10.3390/computers13120339
26. Lenzen, N., Altay, O. (2022), *Machine learning enhanced dynamic response modelling of superelastic shape memory alloy wires*, Materials, 15(1): 304. doi: 10.3390/ma15010304
27. Pawul, M., Śliwka, M. (2016), *Application of artificial neural networks for prediction of air pollution levels in environmental monitoring*, J Ecol. Eng. 17(4): 190-196. doi: 10.12911/22998993/64828
28. Didych, I., Mykytyshyn, A., Stanko, A., Mytnyk, M. (2024), *Application of machine learning methods to the prediction of NO_2 concentration in the air environment*, ITTAP'2024: 4th Int. Workshop on Information Technologies: Theoretical and Applied Problems, 2024, Ternopil, Ukraine, Opole, Poland, CEUR Workshop Proc. 3896: 569-577.
29. Proppe, C., Schuëller, G.I. (2001), *Effects of uncertainties on lifetime prediction of aircraft components*, Proc. First MIT Conf. Comput. Fluid Solid Mech., Cambridge, MA, USA, pp. 425-428.
30. Haykin, S., Neural Networks and Learning Machines, 3rd Ed., Pearson Education Ltd., 2009.
31. Raschka, S., Python Machine Learning: Unlock deeper insights into machine learning with this vital guide to cutting-edge predictive analytics, 1st Ed., Packt Publishing Ltd., 2015. ISBN 978-1-78355-513-0
32. https://xnought.github.io/backprop-explainer/
33. Liu, J., Chen, J., Sun, Z., et al. (2023), *A study on fatigue crack closure associated with the growth of long crack in a new titanium alloy*, Metals, 13(8): 1377. doi: 10.3390/met13081377